

1-1-2000

Spin-Exchange Term in the Solvent Equation of State Near the Critical Point for Electron Transfer Reactions

Juana Vivó Acrivos

San Jose State University, juana.acrivos@sjsu.edu

Follow this and additional works at: https://scholarworks.sjsu.edu/chem_pub

 Part of the [Physical Chemistry Commons](#)

Recommended Citation

Juana Vivó Acrivos. "Spin-Exchange Term in the Solvent Equation of State Near the Critical Point for Electron Transfer Reactions" *Journal Solid of State Chemistry* (2000): 101-110. doi:10.1006/jssc.1999.8629

This Article is brought to you for free and open access by the Chemistry at SJSU ScholarWorks. It has been accepted for inclusion in Faculty Publications, Chemistry by an authorized administrator of SJSU ScholarWorks. For more information, please contact scholarworks@sjsu.edu.

**Spin Exchange Term in the Solvent Equation of State Near the Critical
Point for Electron Transfer Reactions**

J.V. Acrivos*, San José State University, San José CA95192-0101

To the Memory of Kenneth Sanborn Pitzer

Keywords:

*electron spin exchange reactions, equations of state for supercritical metallic,
semi-metallic, polar and non polar solvents*

*Corresponding author:

telephone: 408 924 4972

tele-fax: 408 924 4945

email: jacrivos@athens.sjsu.edu

[www.sjsu.edu /faculty/Acrivos/front.html](http://www.sjsu.edu/faculty/Acrivos/front.html)

Abstract:

Phenomenological Equations of State (EOS) for fluids near their critical point have been obtained using literature compression factor data, $Z_c = P_c V_c / (n R T_c) = 0.40$ to 0.10 in Table I (P_c , V_c/n , T_c are the pressure, volume per n mole, and the absolute temperature of the fluid at the critical point). The objective is to explain the deviations from the van der Waals value, $Z_c(\text{vdW}) = 3/8$ (-70 % for molten Se and alkali metals up to 6 % for molten Pb, Hg, and In) by including in the commonly used phenomenological thermodynamic relations a term which explicitly describes the Heisenberg spin exchange interactions, in order to understand electron transfer reactions in solvents near their critical point. Literature data near the critical point indicate that the $^{199,201}\text{Hg}$ ($Z_c \cong 0.4$) Knight shift plummets to zero while the alkali metals and Se ($Z_c = 0.2$ to 0.1) are paramagnetic fluids, and that the enhanced rates for free radical electron exchange reactions (in CO_2 , $n\text{-C}_2\text{H}_6$ and CHF_3 with intermediate Z_c) are correlated to Z_c . The difference between the solvent behavior for electron spin exchange reactions near its critical point is ascribed to spin interactions. The analysis shows that the solvated electron osmotic pressure in metal ammonia solutions versus the solvent density $\rho_{\text{r,NH}_3} = V_c/V$ goes through a maximum where enhanced rates of electron exchange also attain a maximum. This can be applied to choose the best solvents, near their critical point, for the syntheses of new materials and metal oxide extraction.

Introduction:

Supercritical fluids are used in chemical synthesis due to the increased solubility and chemical reactivity of materials in fluids near and above their critical point¹. Under supercritical solvent conditions, electron exchange reactions must take into account the spin-spin exchange interactions^{2,3}.

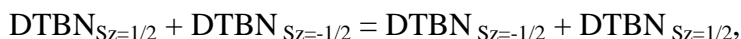
This work is an attempt to use simple and available compression factor data (near the critical point of fluids) to ascertain the contribution to electron exchange reactions of the spin-spin interaction terms going from molten metals, to polar, to non-polar fluids. The deviations from the van der Waals value, $Z_c(\text{vdW}) = 3/8$ in Table I⁴ are the basis for the hypothesis. The gradual change in Z_c between the two extremes Hg ($Z_c \cong 0.4$) to alkali metals and Se ($Z_c \cong 0.2$ to 0.1) is explained in this work, by a semiempirical approach, which adds to the EOS an interaction term that describes the spin exchange interaction explicitly^{5a}. The ^{199,201}Hg Knight shift plummets to zero, and Se dissociates into metallic chains at the critical point^{4d}. Electron spin resonance (esr) measurements at ordinary pressures measure the Heisenberg spin exchange interactions. In the intermediate region, $0.3 \geq Z_c \geq 0.2$, the solvent temperature and pressure dependent spin exchange rate constants^{4h,o} and magnitudes of the free radical isotropic nuclear hyperfine coupling constants⁶⁻⁸ indicate that the solvent is not a passive medium: In alkali metal in ammonia/amine solutions⁶, in most free radical solutions⁷, and in solids⁸ the free electron spin density extends into the surrounding medium. The transferred electron density, n_e/V is proportional to the solvent particle density, n/V surrounding the solute, and the spin exchange energy density varies as^{5a,b} $(n_e/V)^{4/3}$, thus the term which describes the Heisenberg spin interaction varies as $(n/V)^{4/3}$ in the EOS of fluids near the critical point. More accurate EOS (obtained by careful T, V, P measurements) are necessary

to describe the system by scaling concepts⁹⁻¹¹. However, the important question to be answered is what determines the boundaries between metallic, semi-metallic, polar and non-polar solvents for electron transfer reactions in the solvent critical region?

Spin Exchange for Free Radicals in Solution and in Liquid Metals

The extreme variations in Z_c (0.4 for diamagnetic Hg clusters to 0.1 for paramagnetic Se chains^{4c,d}) can not be explained by a simple Lennard-Jones hard spheres approximation. The experimental evidence for intermediate Z_c , (by different type of measurements near the solvent critical point^{4f,h,j,o}) is that there is an enhancement in the electron exchange rates over that calculated by Brownian dynamics simulations, and that this is solvent dependent:

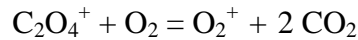
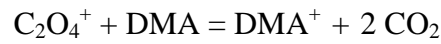
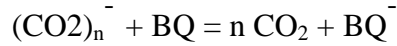
- ESR measurements on di-tert-butyl nitroxide (DTBN) free radical, dissolved in ethane near its critical point ($Z_c = 0.279$ ⁴ⁱ at $T_r = T/T_c = 1.01$, and different $P_r = P/P_c$ reproduced in Figure 1a from ref. 4f) give rates for the spin exchange reaction:



which are faster than can be explained by chemical dynamics' simulations near the critical point^{4f,h,j,k}. The authors obtained extreme variations in the second order rate constants, $k_{ex} = 0.2$ l/mol /ps at $T_r = 1.01$ to 0.05 l/mol /ps at $T_r = 1.08$, and a volume increase to the activated transition state complex for spin exchange, $\Delta V^\ddagger = (\partial \Delta G^\ddagger / \partial P)_T = -RT (\partial \ln k_{ex} / \partial P)_T$ which is much greater than normal fluid activation volumes of 0.05 l/mol. $\Delta V^\ddagger = 7.5$ l/mol at $T_r = 1.01$, $P_r \cong 1.04$ (or 6.3 nm³/DTBN spin exchanged) to 1 l/mol at $T_r = 1.08$, $P_r \cong 1.4$ (or 0.85 nm³/DTBN spin exchanged)^{4f}. The magnitude of the ¹⁴N hyperfine tensor for DTBN goes from 17.2 G in aqueous solutions^{7b} to below 15 G in C₂H₆ near the critical point^{4j}. The variation in the ¹⁴N isotropic hyperfine coupling constant, A_N in the region

where the measured esr reaction rate constants over those calculated by Brownian dynamics' (BD) simulations, $k_{\text{ex,esr}}/k_{\text{ex,BD}}$ attain a maximum, is related to the maximum in the local to bulk solvent density ratio near the free radical, $r_{12} = \rho_{12}^{\text{local}}/\rho_{12}^{\text{bulk}}$ for ethane CO_2 and CHF_3 , (reproduced in Figure 1a for ethane)^{4h}, $r_{12,\text{maximum}}$ depends on the solvent Z_c : $r_{12,\text{maximum}} = -109.93 Z_c + 33.66$ with a residue $R^2 = 0.9999$. Here the ^{14}N spin density dependence on the solvent (T_r , P_r) and the large ΔV^\ddagger for the activated complex indicate that the solvent is involved in the electron exchange reaction.

- The observed kinetics, by transient spectral measurements after pulse radiolysis^{4g,1o} also indicate that the electron exchange rates are enhanced in fluids near their critical point. The rate constants for electron exchange after pulse radiolysis in CO_2 to produce charged free radicals by reaction with p-benzoquinone (BQ), dimethyl aniline (DMA) and O_2 in the reactions^{4g,o}:



are of the same order of magnitude and with a similar dependence on the $\rho_{r,\text{CO}_2} = V_{c,\text{CO}_2}/V$ (Figure 1b) as those reported for DTBN spin exchange in C_2H_6 , CO_2 and CHF_3 ^{4f,j}. The rate constant for reaction with O_2 goes through a maximum just above $\rho_r = 0.5$ whereas the rate constants for BQ and DMA appear to approach a maximum below $\rho_r = 0.5$. The highest enhancement is observed for the formation of BQ^- where our early esr data^{7c} shows that the spin density in p-benzoquinone extends into the solvent to interact with two solvated $^{23}\text{Na}^+$ ions in methanol at ambient pressure.

The object of this work then is to explain the enhanced Heisenberg spin exchange reaction rates by relating the phenomena to the Mott Transition, in order to understand the rate processes involved in the extraction of metal oxides and synthetic chemistry in solvents near their critical point. Spin exchange interactions give rise to the Mott Metal to Insulator Transition where the onset of spin exchange is determined by the simultaneous changes in paramagnetism and metallic behavior³, in alkali metal in ammonia solutions, P doped Si, and in the superconducting cuprates⁶⁻⁸. Additional evidence for enhanced electron transfer near the Mott Transition is given by the ease of organic synthesis in metal-ammonia solutions, and the new metallic compounds achieved in fluids near their critical point¹.

The onset of the Mott Transition at n_{Mott} may be achieved near the solvent critical point, it occurs as the free electron concentration approaches a critical value^{3b}:

$$n_{\text{Mott}} = (0.25/a_{\text{H}})^3, \quad (1)$$

where $a_{\text{H}} = D m_e/m_e^*$ bohr is a hydrogenic radius that depends on the dielectric constant D of the medium and the ratio of the free electron mass to the effective value in the medium, m_e/m_e^* . The effective radius a_{H} varies from an Å for sodium tungstates to over 10^2 Å for InSb and SnTe alloys^{3b}, but it is important to note that the critical concentration n_{Mott} is two orders of magnitude lower than that given by a_{H} . If for a solvent at the critical point $a_{\text{H}} \sim \text{nm}$ then $n_{\text{Mott}} < 1 \text{ M}$ (e.g., solvated electrons and alkali metal in ammonia solutions⁶). Thus the spin exchange term is important for electron transfer chemical reactions that occur in metallic, semi-metallic and polar solvents at concentrations of one spin exchanged per nm^3 (as shown by the reactions^{4f,o} in CO_2 , CHF_3 and C_2H_6). Intermolecular spin flips can be propagated by both dipolar and contact electron-nuclear spin-spin interactions, among the solvent molecules, at the densities obtained near the critical point.

In a many electron system, the spin-spin exchange interaction introduces an energy density term that varies as a function of the transferred electron density, which will be proportional to the solvent density. Thus the additional energy density term, obtained by Thouless for many electron systems^{5a} and by Clementi for molecules^{5b}, is written as:

$$e_{\text{Mott}}/V = -3d(n/V)^{4/3}, \quad (2)$$

where d is a parameter to be determined semi-empirically. The Mott contribution is not expected to be large in polar solvents but it can not be neglected completely, since it is known that the rates of electron exchange are enhanced near the critical point of these solvents^{1,4}. The importance of spin-boson interactions has also been described in the Hamiltonian quantum model for electron transfer processes^{2c}.

Phenomenological Equations of State with Spin Exchange

The three phenomenological relations that are most often used to describe fluids near their critical point are variations of the van der Waals (vdW), the Redlich-Kwong (R-K) and the Anderko-Pitzer (A-P)¹⁰ EOS. The reduced pressure P_r is a function of the reduced volume $V_r = 1/\rho_r$ and the temperature T_r . Semiempirical corrections to the pressure in the ideal gas relation are due to: the finite volume of the fluid molecules, the polar terms which depend on V_r^{-2} , V_r^{-3} , V_r^{-4} , and the spin exchange term introduced in this work, which depends on $V_r^{-4/3}$. The EOS near the critical point may be determined by using the thermodynamic relations that identify the critical point:

$$T_r = V_r = P_r = 1, \quad P_r' = (\partial P_r / \partial V_r)_{T_c} = 0, \quad \text{and} \quad P_r'' = (\partial^2 P_r / \partial V_r^2)_{T_c} = 0,$$

the experimental data in Table I,⁴ and the text book relations for the EOS,¹⁰ with an additional term $-d V_r^{-4/3}$ in relation (3):

$$\begin{aligned}
 P_{r, \text{vdW}} &= T_r \left[\frac{1}{Z_c} - \frac{a_{\text{vdW}}}{T_r V_r} - \frac{Z_c d_{\text{vdW}}}{T_r V_r^2} \right] \\
 P_{r, \text{R-K}} &= T_r \left[\frac{1}{Z_c} - \frac{a_{\text{R-K}}}{T_r V_r} - \frac{d_{\text{R-K}} Z_c}{T_r V_r^2} \right] \\
 P_{r, \text{A-P}} &= T_r \left[\frac{1}{Z_c} - \frac{c_{\text{A-P}}}{V_r} + \frac{a}{V_r^2} + \frac{b}{V_r^3} + \frac{g}{V_r^4} - \frac{d_{\text{A-P}} Z_c}{V_r^4} \right]
 \end{aligned}$$

The textbook values¹⁰ are: $b_{\text{vdW}} = 1/3$, $Z_c(\text{vdW}) = 3/8$, with an internal pressure at $T_r = V_r = 1$:

$$-P_{i,r} = -P_i/P_c = (\partial U_i / \partial V)_{T_c} / P_c = T_r (\partial P_r / \partial T_r)_V - P_r = a_{\text{vdW}} / Z_c(\text{vdW}) = 3$$

when U_i is the internal energy; $a_{\text{R-K}} / Z_c(\text{R-K}) = (1 + 2^{1/3} + 2^{2/3})$, $b_{\text{R-K}} = -1 + 2^{1/3}$ and $Z_c(\text{R-K}) = 1/3$; for spherical molecules at $V_r = T_r = 1$: $b_{\text{A-P}} = 0.25$, $c_{\text{A-P}} = 1.33$, $-(\alpha + \beta + \gamma + c / (1 - b)) = 1.047$, and the temperature dependence of α , β , γ , $b_{\text{A-P}}$ and $c_{\text{A-P}}$ (given explicitly in ref. 10) obtains: $-P_{i,r}(V_r = T_r = 1) = 1.54 / Z_c$. The observed values^{4d}, $-P_{i,r} \text{ experimental}(V_r = T_r = 1) = 3.96$ for Hg and 4.22 for Cs, indicate that $(\partial d / \partial T_r)_{V_c} - d = 1.54 / Z_c + P_{i,r} \text{ experimental}$ is non zero.

The parameters for the three EOS (3) near the critical isotherm were obtained using "Mathematica" version 3.0 notebooks.¹² Typical values are given in Table I together with literature data from various laboratories.⁴ Figure 2 shows the fit of the A-P EOS, determined from a single data point, Z_c to the experimental data^{4a,i} for CO_2 and C_2H_6 near their critical point; the average deviation is 2.5 % for CO_2 , but is not as good for C_2H_6 . The approach to the critical point for extreme values of Z_c , $\text{Ln}|\Delta P_i|$ versus $\text{Ln}|\Delta \rho|$ (when $\Delta P_i = (P_{ic} - P_i) / P_{ic}$ and $\Delta \rho = (\rho_c - \rho) / \rho_c$) for Hg, Cs and Rb gives a slope of one for both the experimental^{4d} and the calculated values. Figure 3 shows plots of the isothermal compressibility, $K_{Tc} = -1/V (\partial V / \partial P)_{Tc}$ obtained from relation (3) versus P_r for different values of Z_c (Hg to NH_3 to Se).

Landau and Zel'dovitch¹³ proposed that there were two transitions near the critical point of gaseous metals, one for the fluid and another for the metal condensation. This hypothesis is

satisfied in the A-P EOS for metals ($0.2 \geq Z_c \geq 0.1$) by imposing 5 boundary conditions in relation (3) to describe the two contiguous phase transitions: $P_r = V_r = T_r = 1$, and $P_r^i = (\partial^i P_r / \partial V_r^i)_{T_c} = 0$ when $i = 1$ to 4.

Results:

The EOS are used to ascertain how the bulk properties of the fluid vary with Z_c :

- Three different regions are identified in Figure 4:
 - $0.10 \leq Z_c \leq 0.2$ identifies a metallic fluid at the critical point.
 - $0.20 \leq Z_c \leq 0.3$ identifies a polar fluid at the critical point.
 - $0.30 \leq Z_c \leq 0.42$ identifies a non-polar fluid at the critical point.
- The difference between the fluid properties are evident in K_{T_c} versus P_r (Figure 3):
 - $K_{T_c}(\text{Hg})$ is fairly symmetric about $P_r = 1$, and of the same order of magnitude as the experimental values^{4c,d} as it goes to infinity when $P_r \Rightarrow T_r = 1$, but as Z_c decreases from Hg to CO_2 to NH_3 to Se, the approach to infinity becomes increasingly asymmetric (Figure 2a, insert for $K_{T_c}(\text{CO}_2)$). Thus, for synthetic work it is useful to note that Se is more compressible than NH_3 than CO_2 than Hg and that all are more compressible below $P_r = 1$ than above it.
- The dependence of the individual contributions in the A-P EOS versus Z_c give some physical insight in Figure 4:

- The energy contributions at the critical point using the Anderko-Pitzer EOS are:

$$E_{\text{polar}} / RT_c = \alpha / V_r,$$

$$E_{\text{hyperpolarizability}} / RT_c = (1/2 \beta / V_r^2 + 1/3 \gamma / V_r^3),$$

$$E_{\text{spin exchange}} / RT_c = -3 d Z_c / V_r^{1/3}$$

- The ratios of the pressure and energy contributions relative to the second order V_r^{-2} terms versus Z_c show negligible contributions from terms in V_r^{-3} plus V_r^{-4} while:

$$\begin{aligned} (P_{\text{exchange}}/P_{\text{polar}})_{Pr = Tr = Vr = 1, 0.2 \leq Z_c \leq 0.42} &= -0.964 Z_c + 0.306 \text{ (residue } R^2 = 0.999), \\ (P_{\text{exchange}}/P_{\text{polar}})_{Pr = Tr = Vr = 1, 0.1 \leq Z_c \leq 0.2} &= -9.40 Z_c + 1.672 \text{ (residue } R^2 = 0.97). \end{aligned} \quad (4)$$

and

$$\begin{aligned} (E_{\text{exchange}}/E_{\text{polar}})_{Pr = Tr = Vr = 1, 0.2 \leq Z_c \leq 0.42} &= -2.959 Z_c + 0.936 \text{ (residue } R^2 = 1), \\ (E_{\text{exchange}}/E_{\text{polar}})_{Pr = Tr = Vr = 1, 0.1 \leq Z_c \leq 0.2} &= -28.25 Z_c + 5.035 \text{ (residue } R^2 = 0.97). \end{aligned} \quad (5)$$

All the energy contributions are an order of magnitude smaller than the fluid Helmholtz free energy, A relative to the standard Gibbs free energy G^0 (Figure 5)¹⁰:

$$\frac{A - G^0}{RT_c} = -1 + \ln \left(\frac{F_c}{Z_c} \right) + \dots$$

The Mott spin exchange contribution to the pressure gives further physical insight into chemical reactivity. The parameter d is a measure of the solvent mediated spin exchange near the critical point. It gives the ability of a solvent to mediate electron spin exchange reactions according to Z_c in Table I:

- Supercritical Se with metallic conductivity^{4d} ($Z_c = 0.105$), up to the alkali metals ($Z_c \leq 0.20$) appear to be the best solvents for electron spin exchange reactions.
- D_2O and methanol ($Z_c = 0.20$) to NH_3 ($Z_c = 0.24$) and CHF_3 ($Z_c = 0.25$) to CO_2 and $n-C_2H_6$ ($Z_c = 0.28$) up to Xe ($Z_c = 0.29$) are the next best solvents.
- H_2 , 4He and Ne ($Z_c = 0.30$) should make no contribution to spin exchange, and.
- Liquid Hg, In and Pb with $Z_c = 0.40$ to 0.36 should to be the worst solvents, near their critical point for electron exchange reactions because of clustering.^{4d} The term $d < 0$ indicates repulsive interactions for expanded Hg, Pb and In. This agrees with the fact that

on the high density side of (T_c, P_c) the Hg conduction is non-metallic and thermally activated, and that the Knight shift plummets to zero, indicating that the electrons are localized in diamagnetic clusters^{4c,d}. The value of Z_c predicts that the same should be true for Pb and In.

The question that remains to be answered is how does the electron osmotic pressure change near the solvent critical point? Thermodynamic data is available^{5c, 6a,b} for the Mott Transition in metal-ammonia solutions at ambient temperatures for $[\text{NH}_3]/[\text{M}] \approx 10^2$, or $\rho_{e,r} \approx 10^{-2} \rho_r$ (where ρ_r is the solvent reduced density and $\rho_{e,r}$ is that for the long lived solvated electron). As the solvent critical point is reached, $a_H^{-3}/\rho(\text{M}) \approx 10$ obtains $\rho(\text{NH}_3) / a_H^{-3} \approx 10$ ($\rho_{H,r} = a_H^{-3} \rho_c(\text{NH}_3)$). Using this data, the electron osmotic pressure has been evaluated using the Debye-Hückel theory and the Mott term in relation (3) for the vdW EOS^{5c}:

$$P_{r, \text{metal-ammonia solution}} = P_{\text{NH}_3} + P_{\text{electrons}} + P_{\text{cations}}$$

where :

$$P_{c,r} = P_{\text{cation}} = \frac{P_{\text{NH}_3}}{Z_c} - P_{\text{cation, correlations}}$$

$$P_{e,r} = P_{\text{electrons}} = \frac{P_{\text{NH}_3}}{Z_c} - P_{\text{electron, correlations}}$$

$$DH = \frac{1}{2} \frac{e^2}{\epsilon_0 \epsilon_r} \frac{1}{r} \quad d_e = 1.5 \quad k_B T_c = \frac{1}{2} \frac{e^2}{\epsilon_0 \epsilon_r} \frac{1}{r} = 1 \quad 6.$$

and the effect of the solvated cation reduced density $\rho_{c,r}$ is neglected, E_F is the Fermi energy,

$DH \rho_{e,r}^{1/2}$ is the contribution introduced in the Debye-Hückel theory, and $d_e \rho_{e,r}^{4/3}$ is the spin exchange term^{5c}. The Debye-Hückel term introduces the effect of local charge structure. Figure 6 shows that the reduced electron osmotic pressure versus the solvent ρ_r , at $T_r = 1$, increases before the solvent critical point is reached near $\rho_r(\text{NH}_3) \cong 0.5$. This is a typical action-reaction effect; an increase in the solvent pressure induces an increase in the electron osmotic pressure. Since the free electron osmotic pressure goes through a maximum near the same density where esr measurements indicate that there is a maximum in the ratio of the local to bulk solvent density^{4j}, and where the Heisenberg spin exchange rate constants also go through a maximum^{4g,f,o} (Figure 1) it follows that the Debye-Hückel approximation can explain measurements which are sensitive to the local solvent structure. The EOS are also correlated to the data:

- The linear correlation between the maximum (which occur for DTBN in CHF_3 , CO_2 and C_2H_6 near $\rho_{r, \text{solvent}} = 0.5$ at $T_r = 1.01^{4j}$) in the local to bulk solvent density ratio around the solute, $r_{12, \text{maximum}}$ versus Z_c (Figure 7a), and between the measured to calculated rate constant ratios, $k_{\text{ex, esr}}/k_{\text{ex, DB}}(\text{DTBN})_{\text{max}}$ versus d (Figure 7b) indicate that the local solvent density enhancement relative to the bulk, the parameter d and the Heisenberg spin exchange interactions are interdependent in Z_c .
- Solvatochromism in fluids near their critical point can be correlated to the relative contributions in the EOS. Interactions with the fluid change the value of the solute optical excitation energy, $h\nu$ relative to that observed in a normal solvent, $h\nu_0$, e.g., cyclohexane. The polarity parameter, reported for N,N-dimethyl-4-nitroaniline in NH_3 and CO_2 ^{4e}, $\pi^* = \pi^* = (\nu - \nu_0)/s$ (where s is a constant) versus the ratio $E_r(\text{CP}) = E_{\text{polar}}/E_{\text{exchange}}$ for the solvent (Figure 7c) indicates that though the spin exchange is expected to be small in polarizable

solvents, π^* does depend on Z_c and increases as the ratio $E_r(\text{CP})$ increases. Here $\pi^* > 0$ indicates that the solute-solvent ground state energy interactions are stronger than in the excited state, whereas $\pi^* < 0$ indicates the reverse⁴ⁿ. In solvents with high polarizability, e.g., NH_3 and CO_2 the dipolar interactions are expected to be highest in the ground state, whereas spin exchange interactions can occur only in the excited state, thus the polar and spin exchange interactions tend to cancel each other so that p^* increases only as $E_r(\text{CP})$ increases (Figure 7c).

Conclusions/Predictions/Use of Phenomenological EOS:

The results indicate that an enhanced solvated electron osmotic pressure near the metal to non-metal transition is related to the enhanced local to bulk solvent density ratio, and to the enhanced free radical spin exchange rate constants, observed near the solvent critical point. This suggests that all these properties are related by a universal truth on the nature of spin exchange contained in Z_c . This should be useful for chemical synthesis as well as metal oxide extraction processes in solvents near their critical point.

Acknowledgements:

The work is dedicated to K.S. Pitzer whose unique insight has left us the Berkeley legacy that Thermodynamic data must be applied using a simple approach. I am grateful to Jean Pitzer for letting me know his thoughts on a preprint of this work that he read. C. Jonah and G. M. Schneider were very kind to send me reprints and preprints of their work that were used to support the model proposed. J.M. Honig gave me most helpful comments. The work was supported by grant NSF-DMR 9612873 and NSF-INT 9312176.

References:

- (a) P.G. Jessop and W. Leitner, *"Chemical Synthesis Using Supercritical Fluids"*, Wiley,-VCH, Germany (1999) ; (b) J.F. Brennecke, D.L. Tomasko and C.A. Eckert, *J. Phys. Chem.*, **94**, 7692 (1994); (c) J. Y. Lu, B.R. Cabrera, T. Wang and J. Li, *Inorg. Chem.*, **37**, 4480 (1998); (d) J. Li, Z. Chen, K. Lam, S. Mulley and D. Proserpio, *Inorg. Chem.*, **36**, 684 (1997); (e) J. Li, Z. Chen, T.J. Emge and D.M. Proserpio, *Inorg. Chem.*, **36**, 1437 (1997); (f) S. Kim and K.P. Johnston, *Ind. Eng. Chem. Res.*, **26**, 1206 (1987); (g) R.I. Cukier and D.G. Nocera, *Ann. Rev. Phys. Chem.*, *H.L. Strauss, ed.*, 49, 337 (1998); (h) R.L. Smith. T. Yamaguchi, T. Sato, H. Suzuki and K. Sato, *Journal of Supercritical Fluids*, **13**, 29 (1998)
- (a) H. Taube, *Electron Transfer Reactions of Complex Ions in Solution*, Academic Press, 1970, NY, London; (b) R. Marcus, *J. Chem. Phys.*, **24**, 966; 979 (1956); (c) P.A. Frantsuzov, *ibid.*, **111**, 2075 (1999)
- (a) N. F. Mott , *Metal to Insulator Transition*, Taylor and Francis, 1974, 1990; (b) N. F. Mott, *Conduction in Non-Crystalline Materials*, Clarendon Press, Oxford (1987), p. 41; (c) A. S. Alexandrov and N.F. Mott, *Polarons and Bipolarons*, World Scientific, London(1995)
- (a) T. Tsuji, S. Honda, T. Hiaki, M. Hongo, *Journal of Supercritical Fluids*, **13**, 15, (1998); (b) W. C. Reynolds, *Thermodynamic Properties in SI*, Published by the Department of Mechanical Engineering: Stanford University (1979); (c) F.Hensel, *Phase Separations in Expanded Metallic Liquids in Physics and Chemistry of Electrons and Ions in Condensed Matter, ed., J.V. Acrivos, N. F. Mott and A. D. Yoffe*, D. Reidel: Dordrecht, 1984, p. 401; (d) F. Hensel and W.W. Warren, *Fluid Metals*, Princeton University Press, Princeton (1999); (e) G.M. Schneider, *Journal of Supercritical Fluids*, **13**, 5 (1998); (f) T.W. Randolph and C. Carlier, *J. Phys. Chem.*, **96**, 5146 (1992) ; (g)N.M. Dimitrijevic, D.M. Bartels, C.D. Jonah and

K. Tahashi, *Chemical Physics Letters*, **309**, 61 (1999); (h) S. Ganapathy, T.W. Randolph, C. Carlier and J.A. O'Brien, *Int. J. of Thermodynamics*, **17**, 471 (1996); (i) B.A. Younglove and J.F. Ely, *J. Phys. Chem. Ref. Data*, **16**, 577 (1987); (j) S. Ganapathy, C. Carlier, T.W. Randolph and J.A. O'Brien, *Ind. Eng. Chem. Res.* **35**, 19 (1996); (k) J.L. deGrazia, T.W. Randolph and J.A. O'Brien, *J. Phys. Chem. A* **102**, 167 (1998); (l) K. Takahashi, S. Sawamura and C. D. Jonah, *Journal of Supercritical Fluids*, **13**, 155 (1998); (m) G. L. Closs, L.T. Calcaterra, N.J. Green, K. W. Penfield and J.R. Miller, *J. Phys. Chem.*, **90**, 3673 (1986); (n) M. Maiwald and G.M. Schneider, *Ber. Bunsenges. Phys. Chem.*, **102**, 960 (1998); (o) N.M. Dimitrijevic, K. Takahashi, D. M. Bartels, C.D. Jonah and A.D. Trifunac, *J. Phys. Chem A*, in press (1999); (p) S.N. Batchelor, *J. Phys. Chem. B* **102**, 615 (1998)

5. (a) D.J. Thouless, *The Quantum Mechanics of Many-Body Systems*", Academic Press, New York (1972); (b) E. Clementi, "*MOTECC*", ESCOM (1991), p.84; (c) J. V. Acrivos, *Phil. Mag.* **52B**, 471 (1985); (d) S. C. Tucker and M. W. Maddox, *J. Phys. Chem. B* **102**, 2437 (1999)

6. (a) C.A. Kraus and W. Lucasse, *J. Am. Chem. Soc.*, **44**, 1949 (1922); (b) J.V. Acrivos, *J. Phys. Chem.*, **88**, 3740 (1984); (c) P.P. Edwards, *ibid.*, **88**, 3772 (1984); (d) G.A. Kenney-Wallace, G.E. Hall, L.A. Hunt and K. Sarantidis, *ibid.*, **84**, 1145 (1980); (e) M. S. Matheson, *Solvated Electron*, R. F. Gould, ed., 1965, p. 47

7. (a) P.P. Edwards, *J. Phys. Chem.*, **84**, 1215 (1980); (b) W. Plachy and D. Kivelson, *J. Chem. Phys.*, **47**, 3312 (1967); (c) J.V. Acrivos, *ibid.*, **47**, 5389 (1967); (d) B.Bales, "*Biological Magnetic Resonance*", **8**, Berliner, ed., Plenum, p. 77 (1990)

8. (a) D. Issa, A. Ellaboudy, R. Janakiraman and J.L. Dye, *J. Phys. Chem.*, **88**, (1984); (b) J.V. Acrivos, *Mol. Cryst.*, **284**, 411 (1996)

9. J.V. Sengers and J.M.H. Levelt Sengers, *Ann. Rev. Phys. Chem.* **37**, 189 (1986)
10. K. S.Pitzer, *Thermodynamics*, Mc Graw Hill Inc, New York (1994)
- 11 (a) A. Anderko, and K.S. Pitzer, *Am. Inst. Chem. Eng. J.*, **1991**, 37, 1379; (b) K.S. Pitzer, *J. Am. Chem. Soc.*, **80**, 5046 (1958); *J. Phys. Chem.*, **77**, 268 (1973); *ibid.*, **88**, 2689 (1984).
12. S. Wolfram, *The Mathematica Book* , Cambridge University Press, 1993
13. (a) L. D. Landau and G.Zel'dovitch, *Acta Phys. Chim. USSR*, **18**, 194 (1943); (b) E. M. Lifshitz and L.D. Landau, *Statistical Physics*, Vol. 1, Pergamom, New York, 1993; E. M. Lifshitz, L. P.Pitaevskii, *Statistical Physics*, Vol. 2, Pergamom, New York, 1980.

Table I: Critical point data taken from ref. 4a (T), 10 (P), 4c, d (H and H&W), 4b (R) and 9 (L&S) together with the EOS parameters obtained from relations (3). Data from different laboratories indicate the accuracy expected. The ratio of energy contributions at the critical point $E_r(\text{CP}) = E_{\text{polar}}/E_{\text{spin exchange}}$ gives the relative importance of the two terms. Unless indicated, the A-P EOS parameters $\alpha = -2.74$, $c = 1.33$ and $b = 0.25$ in ref. 10 are left unchanged to solve (3) for d, β, γ to obtain the pressure and energies in Figure 4 versus Z_c .

FLUID	Experimental Data					A-P EOS			vdW EOS			R-K EOS		
	T _c (K)	P _c (bar)	V _c (cc)	REF.	Z _c	E _r (CP)	α	d	a	b	E _r (CP)	a	b	E _r (CP)
Hg	1750	1671	34.89	H	0.401	-3.8	-2.74	-0.6	1.23	0.34	-3.8	1.74	0.28	-0.8
In	6973	4000	54.67	H&W	0.377									
Pb	5373	2500	64.75	H&W	0.362	-7.6	-2.74	-0.3						
Ne	44.4	27.6	41.70	P	0.312	60	-2.74	0.04						
H ₂	33.2	13	65.00	P	0.306									
4He	5.2	2.275	57.48	R	0.302	33	-2.74	0.09	0.82	0.30	0.9	1.07	0.25	2.1
H ₂ (para)	32.938	12.838	64.29	R	0.301									
Ar	150.86	48.979	74.57	P	0.291	12.7	-2.74	0.24						
Ar	150.7	48.649	77.88	R	0.302									
Kr	209.39	54.96	92.00	P	0.290									
Xe	289.74	58.4	119.50	P	0.290									
methane	190.555	45.988	99.93	R	0.290									
N ₂	126.2	34	89.20	P	0.289									
N ₂	126.21	33.98	89.30	L&S	0.289	11.8	-2.74	0.27						
O ₂	154.6	50.5	73.40	R	0.288									
t-MeAmine	433.2	40.7	254.00	P	0.287									
H ₂ S	373.2	89.4	98.50	P	0.284									
n-C ₂ H ₆	305.34	48.714	145.50	P	0.279	11.30	-2.75	0.29						
C ₃ H ₆	364.75	46.01	180.59	L&S	0.274									
CO ₂	304.21	73.834	94.83	T	0.277									
CO ₂	304.21	73.825	94.43	R	0.276	13.9	-2.76	0.24						
pyridine	620	56.3	254.00	P	0.277									
SO ₂	430.8	78.8	122.00	P	0.268									
C ₂ H ₄	282.346	50.403	121.48	L&S	0.261									
n-C ₈ H ₁₈	568.76	24.87	492.40	P	0.259									
CHF ₃	299.1	48.2	133.30	P	0.258	7.4	-2.76	0.48	0.54	0.26	0.9	0.66	0.22	0.4
NH ₃	406.8	116.27	71.68	R,P	0.246	6.50	-2.77	0.58						
ethanol	513.85	61.37	166.91	B	0.240									
H ₂ O	647.286	220.89	56.83	R	0.233									
H ₂ O	647.07	220.46	55.78	L&S	0.229	5.00	-2.77	0.80						
acetone	508.1	47	209.00	P	0.233									
methanol	566.55	80.92	117.80	B	0.202									
D ₂ O	643.89	216.73	50.61	L&S	0.205									
Cs	2047.79	117.3	316.45	R	0.218	3.4	-2.74	1.21	0.43	0.24	0.6	0.51	0.21	0.3
Cs	1924	92.5	349.74	H&W	0.202									
Rb	2017	124.5	294.72	H&W	0.219									
Rb	2105	133.9	230.84	R	0.177									
Li	3800	970	69.40	R	0.213									
Li	3273	690	63.10	H&W	0.160									
Na	2573	341	111.60	R	0.178									
K	2178	148	217.22	H&W	0.178									
K	2173	167	193.56	R	0.179	3.00	-2.88	1.79						
Mo	14300	5700	33.08	H	0.159	1.6	-2.50	3.3	0.09	0.16	0.1	0.10	0.16	0.03
Se	1888	385	42.68	H&W	0.105	0.50	-1.60	9.3				0.20	0.17	0.1

List of Figures:

Figure 1: Evidence for enhanced electron exchange rate constants of solutes in solvents (CO₂ and in ethane) below their critical point: (a) Correlation between the ratios of experimental to calculated rate constants ($k_{\text{ex,esr}}/k_{\text{ex,BD}}$) to those of local to bulk solvent (1) density around the solute(2), $\rho_{12}^{\text{local}}/\rho_{12}^{\text{bulk}}$ from esr data (ref. 4j). (b) Normalized exchange rate constant for the formation of BQ⁻, DMA⁺ and O₂⁺ after pulse radiolysis in CO₂, $r_k = k_{\text{ex}}(\rho_r)/k_{\text{ex}}(1.5)$ plotted versus ρ_r using the data in ref. 4o.

Figure 2: Z versus P_r near T_c: (a) Experimental data for CO₂ (ref. 4a) are compared to the calculated values at T_r = 1, 1.02, 1.05, insert shows the isothermal compressibility, K_{Tc} for the A-P EOS including the spin-spin exchange; the average deviation is 2.5 %. (b) Experimental data for C₂H₆ and EOS fit near T_r = 1; the fit is worse than for CO₂.

Figure 3: K_{Tc} evaluated from the critical isotherms obtained using relations (3) and the experimental value of Z_c (Table I). Five boundary conditions are used in (3) for Z_c ≤ 0.18). The parameters used are:

NH₃ : **b = 0.26, c = 1.23, a = - 2.77, g = - 0.399, b = 0.47, d = 0.355**

Se : **g = - 0.25, b = - 0.0035, a = - 1.57, d = 10.277, b = 0.22, c = 1.33**

K : **g = - 0.577, b = 0.729, a = - 2.81, d = 2.14, b = 0.27, c = 1.33**

(a) K_{Tc}(Z_c = 0.4). (b) K_{Tc}(Z_c = 0.25 and 0.11). Though the finite volume parameters b(Hg) = 0.25, b(NH₃) = 0.26 and b(Se) = 0.22 are close, the isothermal compressibility K_{Tc} versus P_r,

at $T_r = 1$ shows that Hg is the least compressible and NH_3 is less compressible than Se for a given P_r near the critical point. This may be important for synthesis work near the critical point of fluids.

Figure 4: Contributions to the pressure and to the energy relative to the second order term in the density versus Z_c at the critical point for the A-P EOS from Mo to Hg. b_{A-P} , c_{A-P} , and a were taken from literature values for a given accentric factor w .¹⁰ The linear fit does not depend on the accentric factor w ¹⁰ in relations (4).

Figure 5: $(A-G^0)/RT_c$ for different solvents: $\text{Hg} \geq \text{Mo} > \text{H}_2\text{O} > \text{NH}_3 > \text{CO}_2 > \text{He} > \text{Cs} > \text{C}_8\text{H}_{18}$.

Figure 6: Osmotic pressure for the solvated electron in alkali metal solutions in NH_3 at $T_r(\text{NH}_3) = 1$ and its first derivative relative to V_r , versus $\rho_r(\text{NH}_3)$.

Figure 7: Correlation of the experimental data to the parameters in Table I: . (a) $r_{12,\text{max}} = (\rho_{12}^{\text{local}}/\rho_{12}^{\text{bulk}})_{\text{max}}$ for different solvents (data of ref, 4h) versus Z_c . (b) $(k_{\text{ex,esr}}/k_{\text{ex,BD}})_{\text{max}}$ for DTBN in different solvents (data of ref, 4h) versus d . (c) Polarity parameter π^* for N,N-dimethyl-4-nitroaniline in NH_3 and CO_2 measured by the shifts in the absorption maxima in the fluid under test at ν relative to ν_0 in a normal liquid solvent (cyclohexane): $\pi^* = \pi_i^* = (\nu - \nu_0)/s$ (data of ref. 4e) versus the ratio of polar energy to spin exchange energy at the critical point $E_r(\text{CP}) = E_{\text{polar}}/E_{\text{spin exchange}}$.

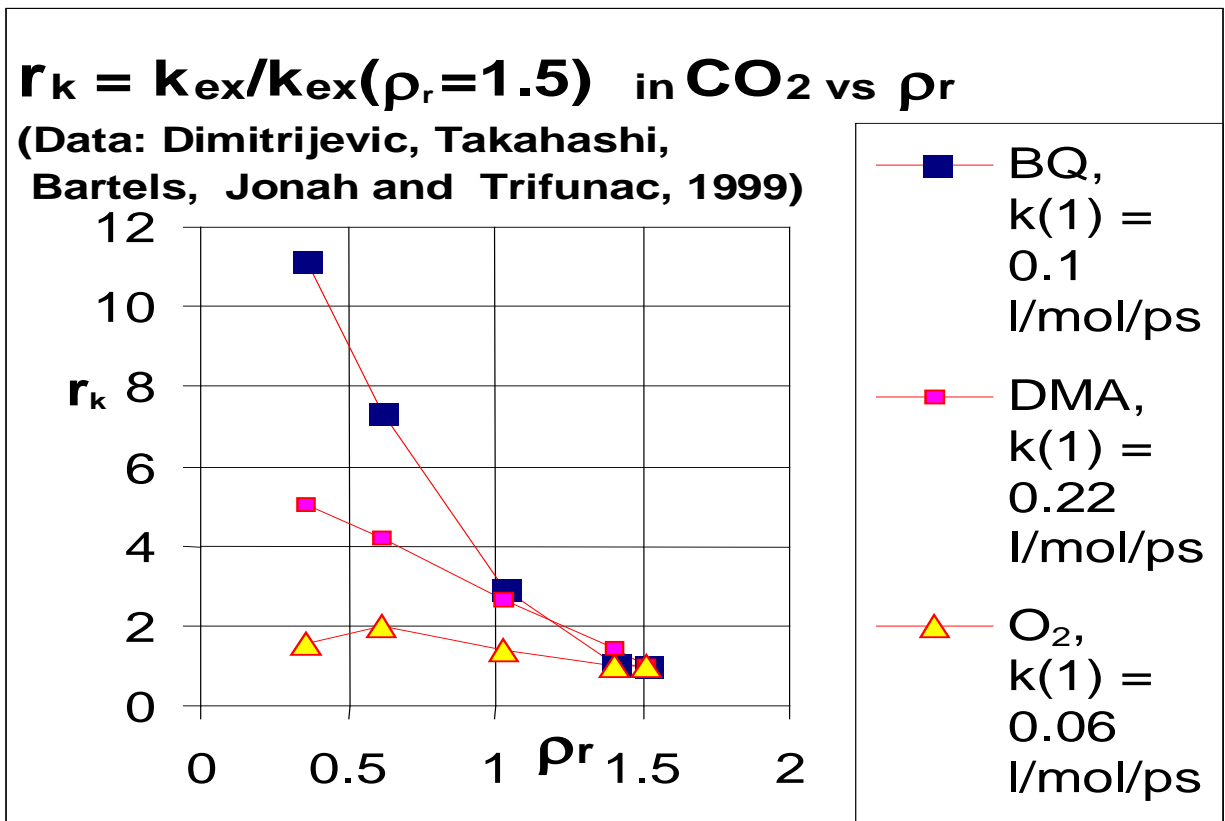


Figure 1b

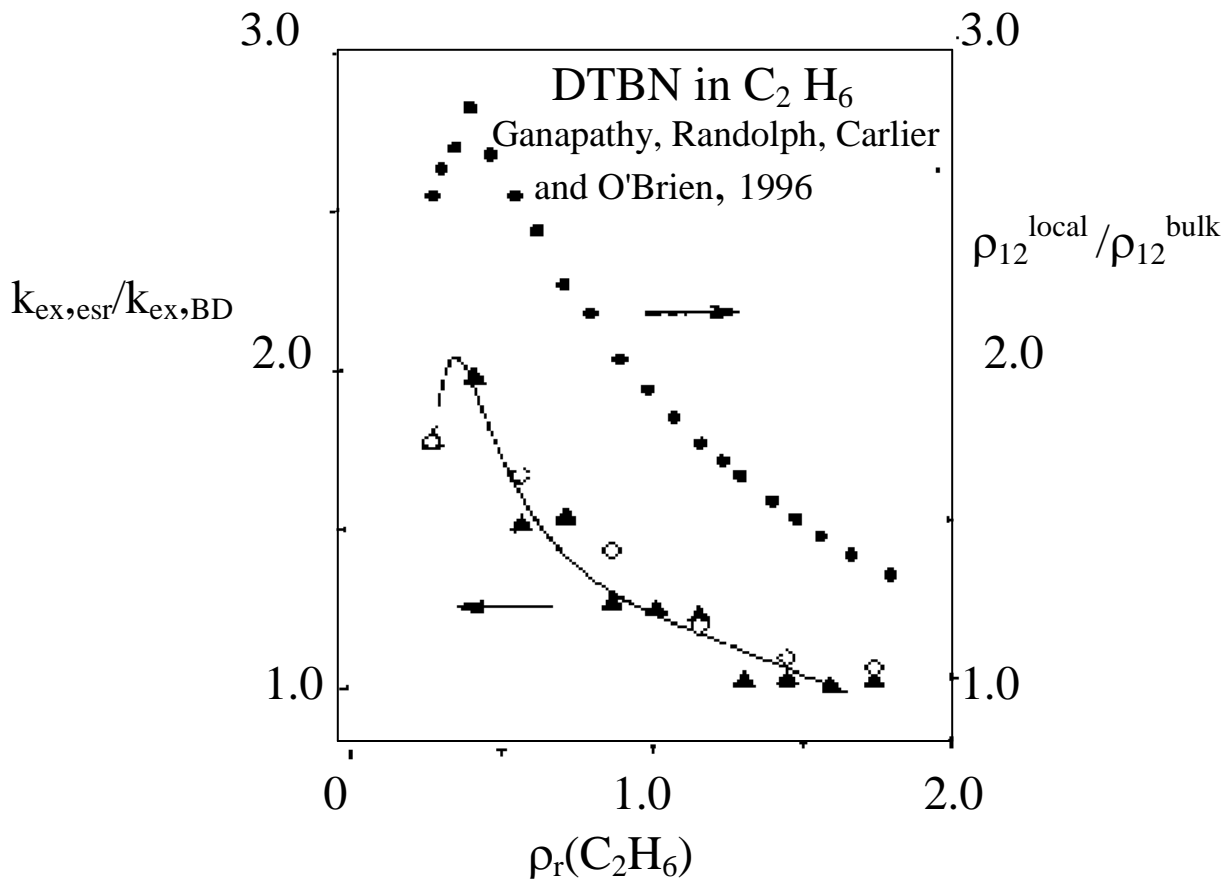


Figure 1a

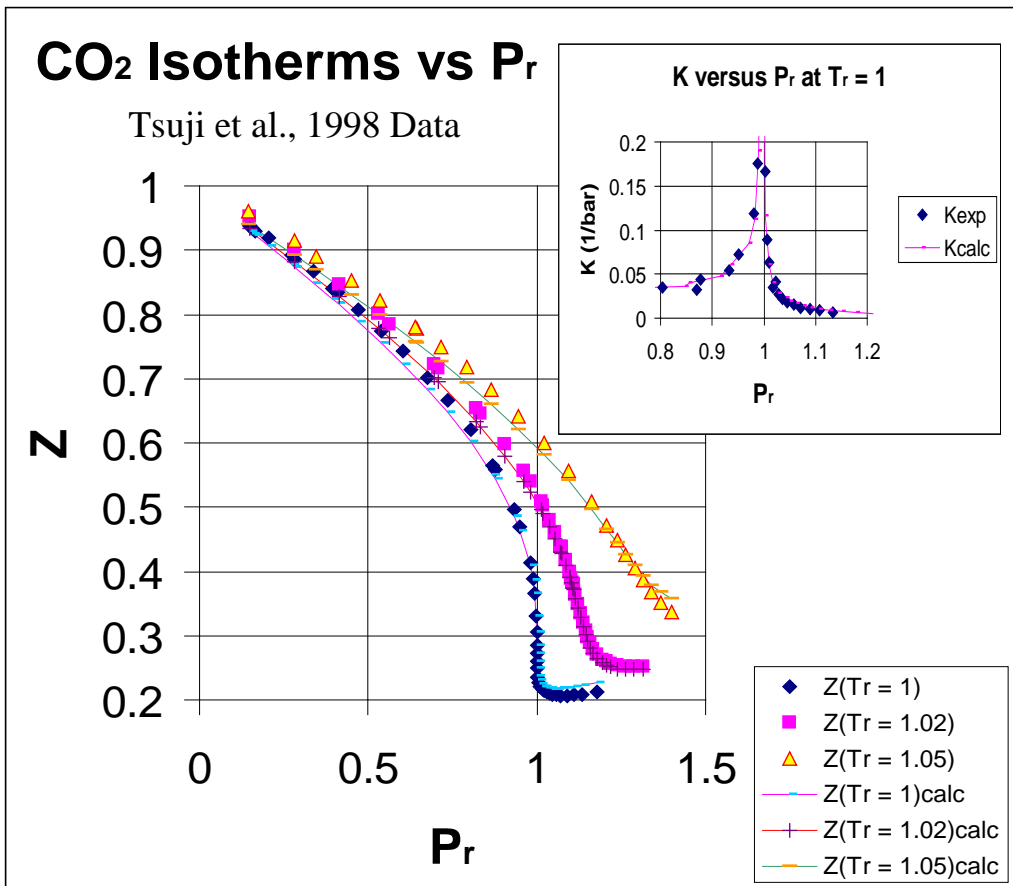


Figure 2a

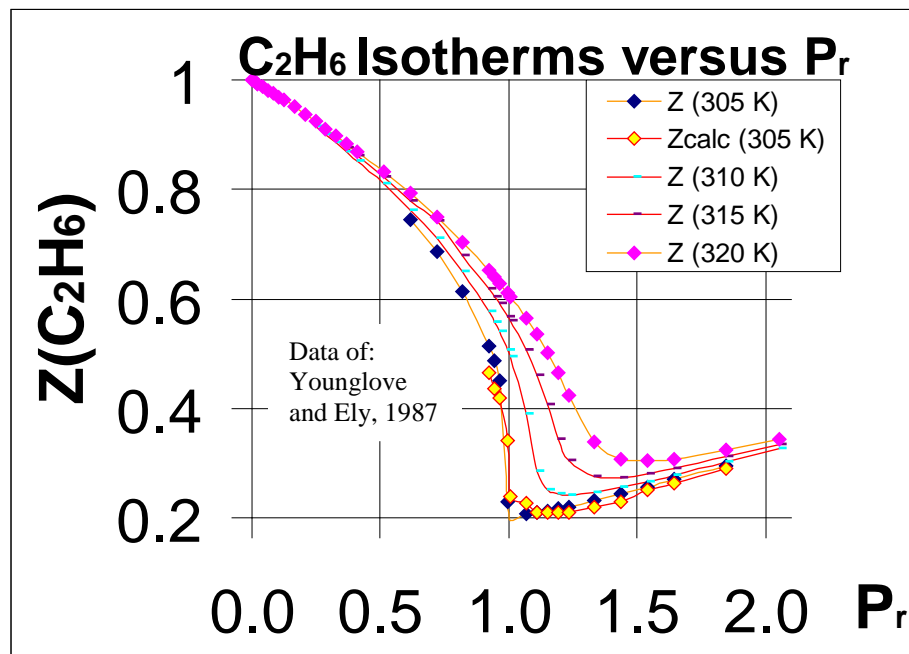


Figure 2b

Figure 3a

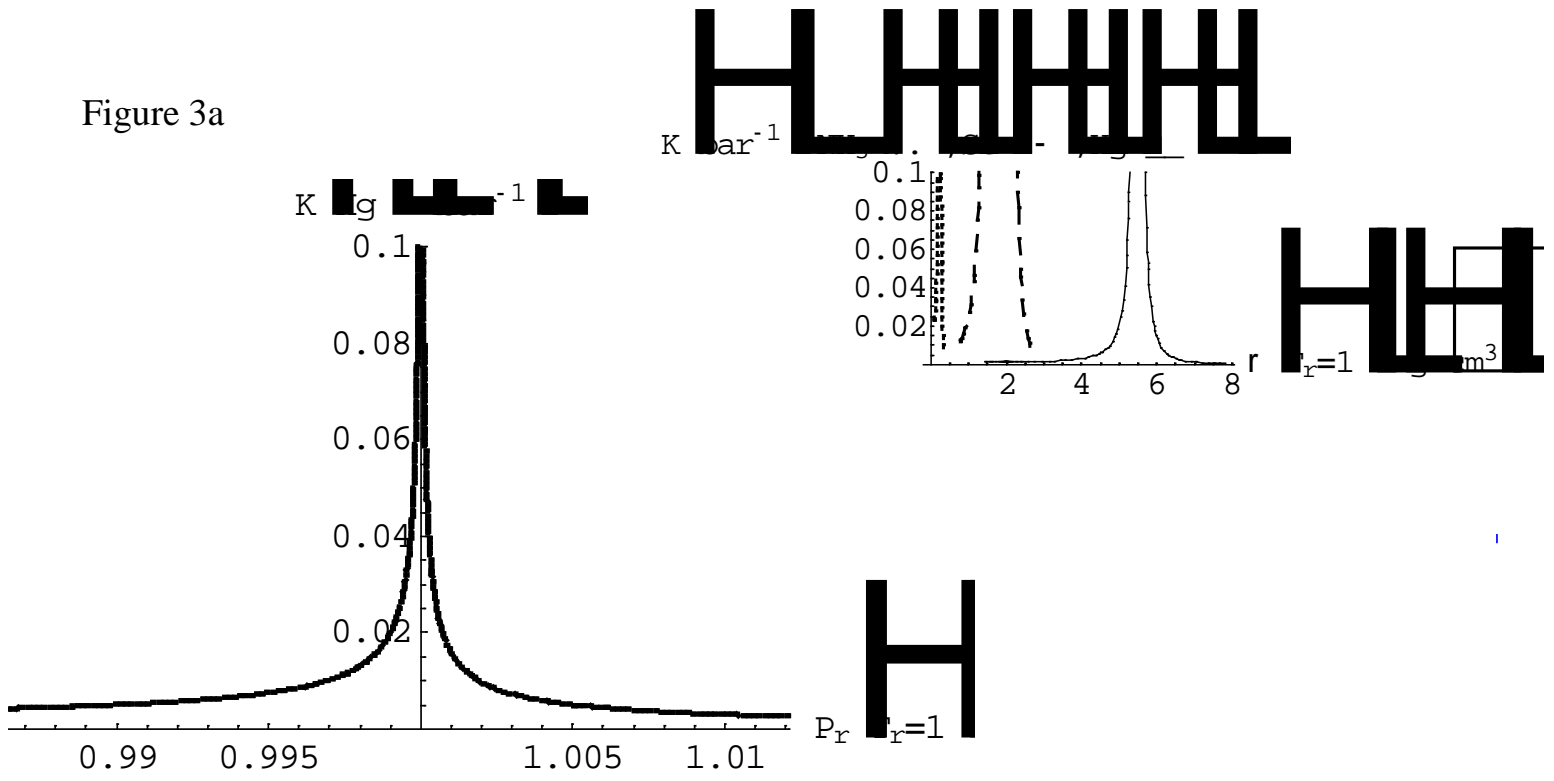
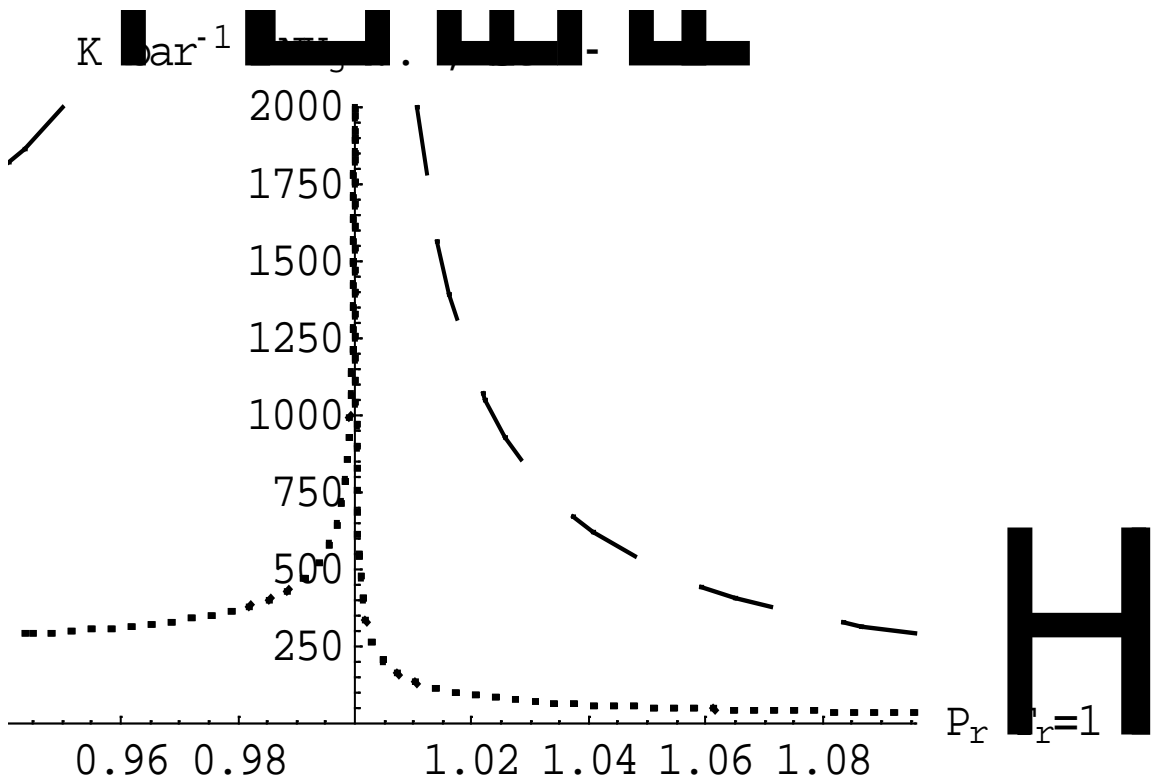


Figure 3b



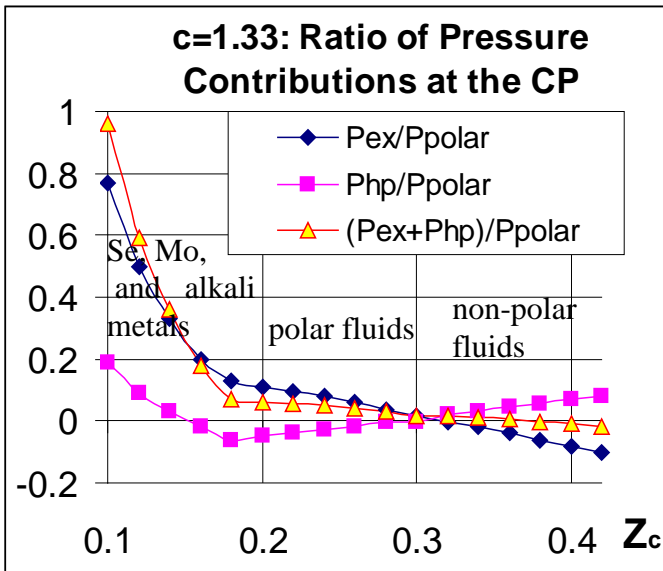
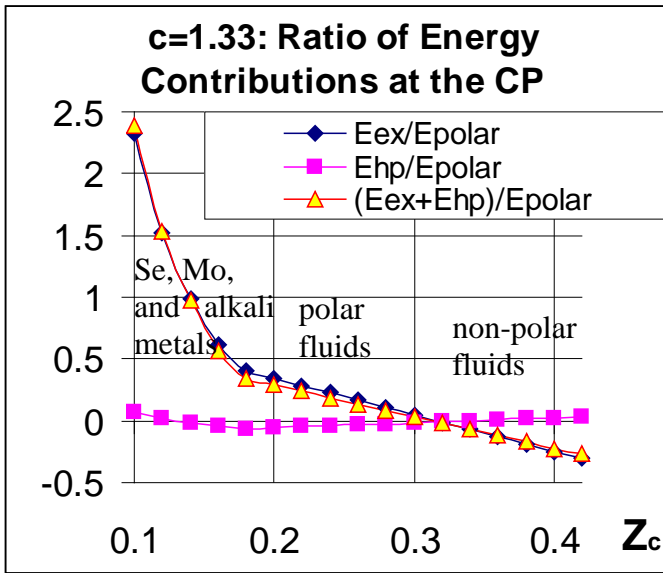


Figure 4

G^0 ρ , ρ_0 , Hg Polar Fluids > Alkali Metals

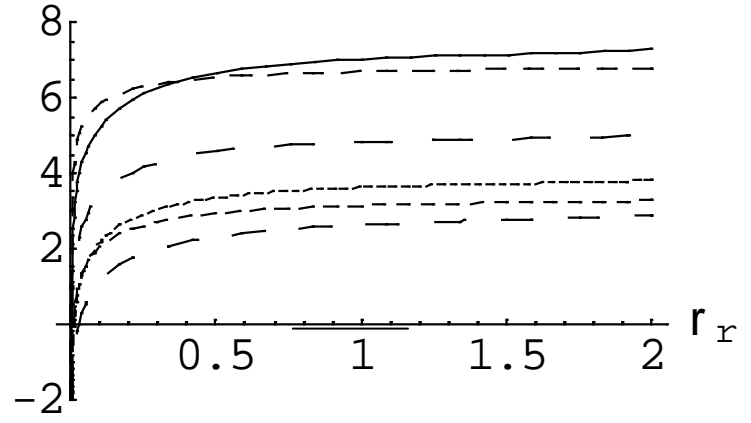


Figure 5

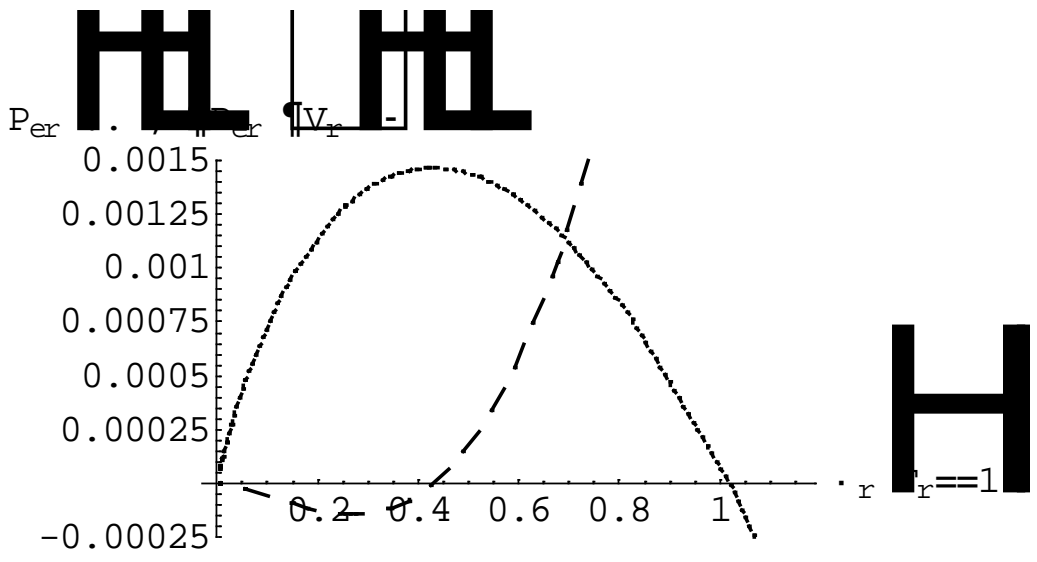


Figure 6

Polarity Parameter π^* , Schneider, 1998

Figure 7c

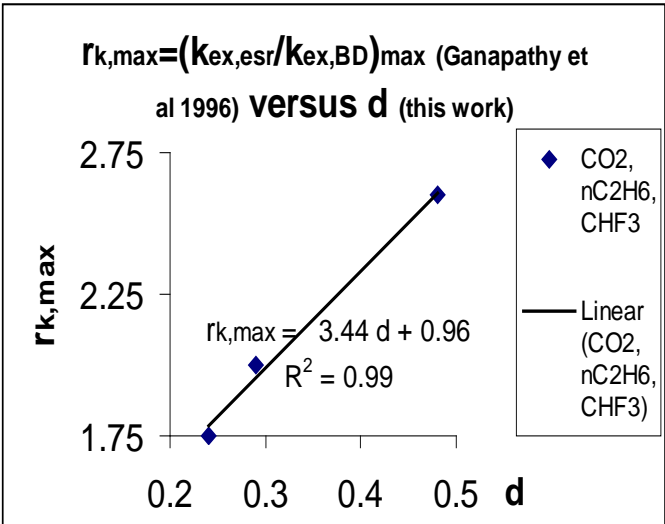


Figure 7b

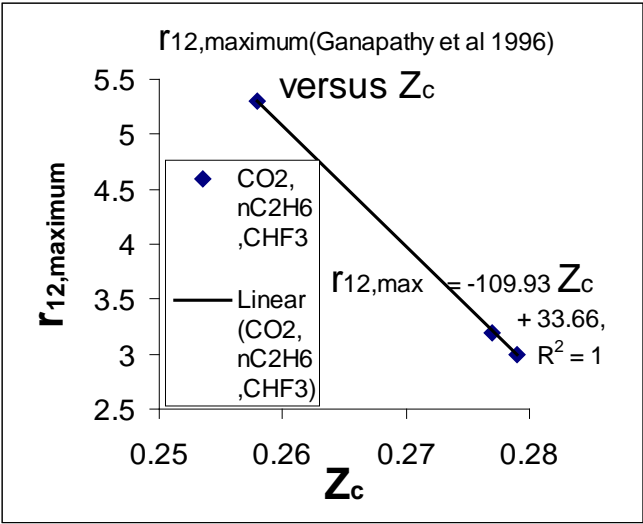


Figure 7a

